

This is an Open Access document downloaded from ORCA, Cardiff University's institutional repository:<https://orca.cardiff.ac.uk/id/eprint/155362/>

This is the author's version of a work that was submitted to / accepted for publication.

Citation for final published version:

Lyu, Xiaowei, Luo, Zhiwen , Shao, Li, Awbi, Hazim and Lo Piano, Samuele 2023. Safe CO2 threshold limits for indoor long-range airborne transmission control of COVID-19. Building and Environment 234 , 109967. 10.1016/j.buildenv.2022.109967

Publishers page: <http://dx.doi.org/10.1016/j.buildenv.2022.109967>

Please note:

Changes made as a result of publishing processes such as copy-editing, formatting and page numbers may not be reflected in this version. For the definitive version of this publication, please refer to the published source. You are advised to consult the publisher's version if you wish to cite this paper.

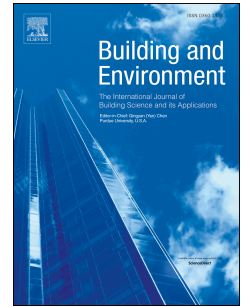
This version is being made available in accordance with publisher policies. See <http://orca.cf.ac.uk/policies.html> for usage policies. Copyright and moral rights for publications made available in ORCA are retained by the copyright holders.



# Journal Pre-proof

Safe CO<sub>2</sub> threshold limits for indoor long-range airborne transmission control of COVID-19

Xiaowei Lyu, Zhiwen Luo, Li Shao, Hazim Awbi, Samuele Lo Piano



PII: S0360-1323(22)01197-0

DOI: <https://doi.org/10.1016/j.buildenv.2022.109967>

Reference: BAE 109967

To appear in: *Building and Environment*

Received Date: 15 October 2022

Revised Date: 16 December 2022

Accepted Date: 29 December 2022

Please cite this article as: Lyu X, Luo Z, Shao L, Awbi H, Lo Piano S, Safe CO<sub>2</sub> threshold limits for indoor long-range airborne transmission control of COVID-19, *Building and Environment* (2023), doi: <https://doi.org/10.1016/j.buildenv.2022.109967>.

This is a PDF file of an article that has undergone enhancements after acceptance, such as the addition of a cover page and metadata, and formatting for readability, but it is not yet the definitive version of record. This version will undergo additional copyediting, typesetting and review before it is published in its final form, but we are providing this version to give early visibility of the article. Please note that, during the production process, errors may be discovered which could affect the content, and all legal disclaimers that apply to the journal pertain.

© 2022 Published by Elsevier Ltd.

1 Manuscript revised to Building and Environment, Dec 2022

2

## 3 **Safe CO<sub>2</sub> Threshold Limits for Indoor Long-range Airborne Transmission**

### 4 **Control of COVID-19**

5 Xiaowei Lyu<sup>1</sup>, Zhiwen Luo<sup>2\*</sup>, Li Shao<sup>1</sup>, Hazim Awbi<sup>1</sup>, Samuele Lo Piano<sup>1</sup>

6 1. School of the Built Environment, University of Reading, UK

7 2. Welsh School of Architecture, Cardiff University, UK

8 Correspondence: Prof Zhiwen Luo (LuoZ18@Cardiff.ac.uk)

9 **Abstract:** CO<sub>2</sub>-based infection risk monitoring is highly recommended under the current  
10 COVID-19 pandemic. However, the CO<sub>2</sub> monitoring thresholds proposed in the literature are  
11 mainly for spaces with fixed occupants. Determining CO<sub>2</sub> threshold is challenging in spaces  
12 with changing occupancy due to the co-existence of quanta and CO<sub>2</sub> remaining from the  
13 previous occupants. Here, we propose a new calculation framework to derive safe excess CO<sub>2</sub>  
14 thresholds (above outdoor level),  $C_t$ , for various spaces with fixed/changing occupancy and  
15 analyze the uncertainty entailed. Common indoor spaces were categorized into three scenarios  
16 according to their occupancy condition, e.g., fixed or varying infection ratios  
17 (infectors/occupants). We proved that rebreathed fraction-based model can be directly applied  
18 for  $C_t$  derivation in the cases of a fixed infection ratio (Scenario 1 and Scenario 2). In the case  
19 of varying infector ratios (Scenario 3),  $C_t$  derivation has to follow the general calculation  
20 framework due to the existence of initial quanta/excess CO<sub>2</sub>. Otherwise, significant bias can be

21 caused for  $C_t$  (e.g., 260 ppm) when infection ratio varies remarkably.  $C_t$  significantly varies  
 22 with specific space factors such as occupant number, activities, and community prevalence,  
 23 e.g., 7 ppm for gym and 890 ppm for lecture hall, indicating  $C_t$  should be determined on a case-  
 24 by-case basis. An uncertainty of  $C_t$  up to 6 orders of magnitude was found for all cases due to  
 25 uncertainty in emissions of quanta and  $CO_2$ , thus emphasizing the role of accurate emissions  
 26 data in obtaining  $C_t$ .

27

28 **Keywords:** infection risk control,  $CO_2$  monitoring, initial quanta, uncertainty analysis

29

### Nomenclature

$B$	Breathing rate, m <sup>3</sup> /h
$C_{CO_2,i}$	$CO_2$ concentration for occupancy stage $i$ , ppm
$C_{cin,i}$	Initial $CO_2$ concentration for occupancy stage $i$ , ppm
$C_{q,i}$	Quanta concentration for occupancy stage $i$ , quanta/m <sup>3</sup>
$C_{qin,i}$	Initial quanta concentration for occupancy stage $i$ , quanta/m <sup>3</sup>
$C_t$	Safe excess $CO_2$ threshold, ppm
$C_{t50}$	Median safe excess $CO_2$ threshold, ppm
$E_{co_2}$	$CO_2$ emission rate, mL/s
$E_q$	Quanta emission rate, quanta/h
$I_i$	Infector number for occupancy stage $i$
$N_{ave}$	Average occupant number
$N_i$	Occupant number for occupancy stage $i$
$P_i$	Infection risk for occupancy stage $i$
$P_t$	Predefined infection risk threshold
$P_l$	Community prevalence
$T_i$	Exposure time for occupancy stage $i$ , h
$V$	Space volume, m <sup>3</sup>
$\lambda_i$	Air change rate for occupancy stage $i$ , h <sup>-1</sup>

30

## 31 1. Introduction

32 COVID-19, as a novel coronavirus disease, has caused a worldwide pandemic spreading  
33 since the end of 2019 (Chen et al., 2020). Indoor transmission control is the key to prevent the  
34 spread of the SARs-CoV-2 virus due to a higher transmission risk indoors than outdoors (Qian  
35 et al., 2020). The four main transmission routes in indoor environments are droplet-borne,  
36 fomite, short-range airborne, and long-range airborne (Li, 2021; Wei and Li, 2016). Although  
37 short-range airborne transmission route was inferred to be the dominant route in close contact  
38 (Chen et al., 2020), long-range airborne transmission was revealed to more likely induce  
39 outbreaks in poorly ventilated and confined indoor spaces (Peng et al., 2022). Thus, it is of  
40 primary importance to monitor and control long-range airborne transmission for indoor  
41 environment.

42 The exhaled infectious aerosols contributing to long-range airborne transmission are difficult  
43 to detect, and can travel a long distance in indoor environment. Therefore, a detectable indicator  
44 for transmission risk is urgently needed to effectively monitor long-range airborne transmission.  
45  $CO_2$  that can be easily monitored through low-cost sensors (Peng and Jimenez, 2021) has been  
46 recommended as risk indicator for long-range airborne transmission because it can both reflect  
47 the indoor ventilation condition and the quanta concentration (Persily et al, 2022). Accordingly,  
48 safe  $CO_2$  thresholds are defined as the maximum  $CO_2$  concentration level under which the  
49 indoor space is at an acceptable infection risk. Such information is useful to guide the design  
50 of infection-resilient buildings.

51 Treating  $CO_2$  as an indicator for indoor ventilation performance, recent studies made use of  
52  $CO_2$  thresholds for risk control based on prevailing ventilation standards with a target of  
53 acceptable indoor air quality (IAQ) but not infection risk (CIBSE, 2021; SAGE-EMG, 2021;

54 REHVA, 2021). ASHRAE does not recommend a specific value of threshold (Persily et al.,  
55 2022), although other organizations have suggested specific thresholds of 800 ppm (SAGE-  
56 EMG, 2020; CDC, 2021) or 800-1000 ppm (REHVA, 2021) to ensure a safe indoor  
57 environment. However, whether a fixed  $CO_2$  threshold could guarantee a low infection risk  
58 for all spaces is questionable considering factors such as occupancy level and respiratory  
59 activity can all affect the value of it (Peng and Jimenez, 2021).

60 Moving beyond the assessment of  $CO_2$  as a mere indicator of indoor ventilation condition,  
61  $CO_2$  can also be used to directly reflect quanta concentration as  $CO_2$  and virus-laden aerosols  
62 can be co-produced and co-inhaled by human. Therefore,  $CO_2$  thresholds can be calculated  
63 backward by pre-defining an acceptable infection risk level (Hou et al., 2021; Peng and  
64 Jimenez, 2021). Indoor airborne transmission risk can be maintained under the predefined risk  
65 level in as much indoor  $CO_2$  concentration can be maintained below the derived threshold.  
66 Occupancy level and respiratory activity for a particular indoor space can all be factored in this  
67 backward calculation process (Hou et al., 2021; Peng and Jimenez, 2021; Rudnick and Milton,  
68 2003). In the literature, the derived thresholds were found to be highly sensitive to factors such  
69 as activity level and community prevalence, making  $CO_2$  thresholds varying across different  
70 indoor spaces (Peng and Jimenez, 2021). For example, the reference excess  $CO_2$  threshold  
71 (above outdoor level) for classroom amounts to only about 150 ppm, while this figure is ten-  
72 fold for supermarket (Peng and Jimenez, 2021). This indicates that the  $CO_2$  thresholds should  
73 be determined case by case, instead of setting a fixed value for all spaces.

74 In addition, most proposed thresholds are for spaces with fixed occupancy level under the  
75 assumption of no initial quanta/excess  $CO_2$  (Hou et al., 2021; Peng and Jimenez, 2021; Rudnick

76 and Milton, 2003). For spaces with variable occupancy, some of quanta/ $CO_2$  released by the  
77 previous group of occupants can remain in the space and become initial quanta/ $CO_2$  when the  
78 next group occupies the space, hence increasing the infection risk for the current occupants.  
79 The initial quanta is essential for defining  $CO_2$  threshold, but it is difficult to estimate as it  
80 requires information of ventilation condition and occupancy profile of previous occupancy  
81 stage. Hence, how to account for initial quanta/excess  $CO_2$  in spaces with changing occupancy  
82 in infection risk assessment remains an unsolved question (Mittal et al., 2020b; Wei and Li,  
83 2016).

84 Finally, emissions of quanta and  $CO_2$  are two important parameters in determining the  $CO_2$   
85 threshold, but they have inter-individual variation and can also be affected by factors such as  
86 age and gender (Buonanno et al., 2020a; Persily and de Jonge, 2017; Good et al., 2021). For  
87 instance, the viral load of super-spreader can be 10 times higher than the mean level of normal  
88 infectious subjects (Lelieveld et al., 2020), which may indicate a higher quanta emission (Ke  
89 et al., 2021, 2022). Different values of quanta and  $CO_2$  emission were adopted by previous  
90 studies for  $CO_2$  threshold derivation, e.g., from 0.37 quanta/h to 100 quanta/h for classrooms  
91 (Buonanno et al., 2020a; Bazant et al., 2021; Hou et al., 2021; Peng and Jimenez, 2021). The  
92 effect on the uncertainty on the emissions of quanta and  $CO_2$  on defining a  $CO_2$  threshold  
93 should be further analyzed. The present study aims to provide a new calculation framework to  
94 derive safe excess  $CO_2$  thresholds ( $C_i$ ) by considering initial quanta/excess  $CO_2$  and  
95 changing/fixed occupancy patterns for different indoor spaces, as well as propagating the  
96 uncertainty of these input variables.

## 97 **2. Methodology**

98 *2.1 General calculation framework*

99 Our model is based on four assumptions for indoor mass balance equations for  $CO_2$  and  
 100 quanta (Hou et al., 2021): 1) both  $CO_2$  and quanta are well mixed and evenly distributed in  
 101 the air; 2) indoor excess  $CO_2$  is released by human exhalation only, with no other indoor  
 102 sources; 3)  $CO_2$  emission rate and quanta emission rate are both constant (i.e., not time  
 103 dependent); 4) the loss of quanta is mainly due to ventilation, other elimination mechanisms  
 104 such as deposition, filtration and inactivation are neglected.

105 In deriving  $C_t$  for spaces with changing occupants, we consider a sequence of occupancy  
 106 stages,  $S_i(I_i, N_i, T_i)$ . Stage  $i$  represents an indoor space (with the volume of  $V$ ) being occupied  
 107 by a number of occupants ( $N_i$ ) with infectors ( $I_i$ ) for a duration of time ( $T_i$ ).  $i=1$  represents the  
 108 start of the occupancy:  $N_1$  occupants (with  $I_1$  infectors) stay in this indoor space for a period of  
 109  $T_1$ , with no people inside prior to  $N_1$  occupants. The introduction of various occupancy stages  
 110 aims to consider the virus released and still in the air from previous occupancy stages (the  
 111 initial quanta). This is fundamentally different from previous studies which only considered  
 112 one-off occupancy or fixed occupancy throughout the exposure period of interest.

113 The general calculation process of  $C_t$  for one occupancy stage of a space is given as follows.

114 Long-range transmission risk for occupancy stage  $i$  is modeled through a Wells-Riley model  
 115 (Riley et al., 1978) amended by Gammitoni and Nucci (1997) to assess infection risk through  
 116 unsteady-state quanta concentration:

$$117 \quad P_i = 1 - e^{-B \int_0^{T_i} C_{q,i}(t) dt} \quad (1)$$

118 Quanta concentration in Equation (1) is modeled through transient mass balance equation:

$$119 \quad \frac{dC_{q,i}}{dt} = \frac{I_i E_q}{V} - \lambda_i C_{q,i} \quad (2)$$

120 Equation (2) can be analytically solved as:

$$121 \quad C_{q,i}(t) = \left( C_{qin,i} - \frac{I_i E_q}{\lambda_i V} \right) e^{-\lambda_i t} + \frac{I_i E_q}{\lambda_i V} \quad (3)$$

122 To control transmission risk of stage  $i$  under an acceptable low level, a risk threshold of  $P_t$   
 123 needs to be initially determined. Based on  $P_t$ , a required ACH (air change rate,  $\lambda_i$ ) can be  
 124 derived by substituting Equation (3) into Equation (1),  $\lambda_i$  should be no less than the derived  
 125 value to keep transmission risk under  $P_t$ .

126 Indoor excess  $CO_2$  concentration is also dominated by ACH, hence it reflects the ventilation  
 127 condition of stage  $i$ .

128 Indoor excess  $CO_2$  concentration for stage  $i$  is determined by mass balance equation (4):

$$129 \quad \frac{dC_{CO_2,i}}{dt} = \frac{N_i E_{CO_2}}{V} - \lambda_i C_{CO_2,i} \quad (4)$$

130 Equation (4) is solved as:

$$131 \quad C_{CO_2,i}(t) = \left( C_{Cin,i} - \frac{N_i E_{CO_2}}{\lambda_i V} \right) e^{-\lambda_i t} + \frac{N_i E_{CO_2}}{\lambda_i V} \quad (5)$$

132 Substituting the required ACH that is backward calculated from transmission risk threshold  
 133 into Equation (5), the time-averaged indoor excess  $CO_2$  concentration ( $C_{CO_2,i}$ ) during  $T_i$  is  
 134 exactly  $C_t$  for stage  $i$  (Hou et al., 2021; Bazant et al., 2021):

$$135 \quad C_t = \frac{1}{T_i} \int_0^{T_i} C_{CO_2,i}(t) dt \quad (6)$$

136 When indoor excess  $CO_2$  concentration is below the reference threshold  $C_t$ , sufficient  
 137 ventilation can be promised to keep long-range transmission risk for occupancy stage  $i$  under  
 138 the risk level of  $P_t$ .

139 Further, for different occupancy stages,  $C_t$  can be derived by following the steps mentioned  
 140 above considering the existence of initial quanta/excess  $CO_2$ , see Equation (3) and Equation  
 141 (5). Starting from occupancy stage 1 without initial quanta/excess  $CO_2$ , a required ACH ( $\lambda_i$ )

142 can be easily obtained following the general calculation process. For occupancy stage 2, the  
143 initial quanta and initial excess  $CO_2$  can be estimated based on the ACH derived in occupancy  
144 stage 1 ( $\lambda_1$ ) under the assumption that excess  $CO_2$  during occupancy stage 1 has been controlled  
145 under the reference threshold,  $C_t$  for occupancy stage 2 can then be obtained according to the  
146 calculation framework. Repeating these steps, i.e. by taking the derived ACH of previous  
147 occupancy stage to estimate initial quanta/excess  $CO_2$  for present stage,  $C_t$  can be calculated  
148 iteratively for all the occupancy stages modeled.

### 149 *2.1.1 Infection Risk Threshold $P_t$*

150 The infection risk threshold  $P_t$  is of great importance as it dominates the safety levels of the  
151 indoor environment. It can be defined in two ways, either by using a constant value for all  
152 environment - such as 1%, 0.1% (Dai and Zhao, 2020) or even 0.01% (Peng and Jimenez -  
153 2021) or to determine  $P_t$  based on reproductive number ( $R_A$ ) where  $R_A$  is the average number  
154 of secondary cases caused by one infector in a given susceptible population in indoor  
155 environment. In the latter, the value of  $P_t$  is dominated by the number of occupants and can be  
156 a large and inconvincible value when occupant number is small (Ma et al., 2018; Furuya et al.,  
157 2009). In this study, we use a constant value of  $P_t = 0.01\%$  as suggested in Peng and Jimenez  
158 (2021), which is reasonable for most occupancy stages when the number of occupants is less  
159 than 10,000.

### 160 *2.2 Designed Scenarios*

161 Three scenarios were identified to calculate  $C_t$ :

162 1) Regularly attended space with fixed occupancy level and the same group of people as  
 163 occupants, so that  $N_1=N_2=...$  (e.g., a lecture room used by a certain group of students)  
 164 (Burridge et al., 2021; Vouriot et al., 2021) ;

165 2) Non-regularly attended space with constant infection ratio ( $I_1/N_1=I_2/N_2=...=I_i/N_i$ ),  
 166 different groups of people as occupants, and with high occupancy level (e.g., shopping center,  
 167 train station);

168 3) Non-regularly attended space with changing infection ratio ( $I_1/N_1 \neq I_2/N_2 \neq ... \neq I_i/N_i$ ) and low  
 169 occupancy level (e.g., gym, train coach).

170 All these scenarios are widely experienced in real-life situations.

### 171 2.2.1 Scenario 1: Regularly attended spaces

172 We determined the number of infectors  $I_i$  for Scenario 1 according to both the indoor  
 173 occupancy level ( $N_i$ ) and local community prevalence ( $P_I$ ). The expected  $I_i$  is defined as max  
 174  $\{1, P_I N_i\}$ . When with a low indoor occupancy level or a low community prevalence, the value  
 175 of  $P_I N_i$  can be less than 1, under such condition,  $I_i$  is assumed to be equal to 1, Otherwise,  $I_i$  is  
 176 assumed to be  $P_I N_i$  to reflect the real local infection condition.

177 Derived from mass balance equations, quanta concentration and excess  $CO_2$  concentration  
 178 were found to have a constant proportion during all the occupancy stages, only affected by  
 179 infection ratio and emissions, see Equation (7) (Full derivation details can be found in  
 180 Supplementary Information). As long as the infection ratio and emissions do not change during  
 181 the occupancy stages, the proportion remains unchanged as well, hence:

$$\frac{C_{q,1}(t)}{C_{CO_2,1}(t)} = \frac{C_{q,2}(t)}{C_{CO_2,2}(t)} = \dots = \frac{I_i}{N_i} \frac{E_q}{E_{CO_2}} \quad (7)$$

Under these circumstances, infection risk for stage  $i$  Eq (1) can be revised as below

$$P_i = 1 - e^{-B \frac{I_i}{N_i} \frac{E_q}{E_{CO_2}} \int_0^{T_i} C_{CO_2,i}(t) dt} \quad (8)$$

Equation (8) can be treated as the classical rebreathed fraction (RF) -based infection risk model derived by Rudnick and Milton (2003), with  $BC_{CO_2,i}(t)/E_{CO_2}$  representing the rebreathed fraction. This derivation proved that rebreathed fraction (RF) -based model can account for the impact of initial quanta/excess  $CO_2$  in risk assessments for spaces with fixed occupants.

Based on Equation (8), the time averaged value  $C_t$  for occupancy stage  $i$  can then be derived as:

$$C_t = \frac{E_{CO_2} N_i}{E_q T_i B I_i} \ln \left( \frac{1}{1 - P_t} \right) \quad (9)$$

### 2.2.2 Scenario 2: Non-regularly attended spaces with constant infection ratios

In Scenario 2, we assumed that community prevalence ( $P_t$ ) can be directly used to represent indoor infection ratio due to the high occupancy level ( $I_1/N_1 = I_2/N_2 = \dots = P_t$ ). The proportion between  $C_{q,i}$  and excess  $C_{CO_2,i}$  also become constant due to the constant infection ratio among occupancy stages (Detailed derivation process can be found in Supplementary Information):

$$\frac{C_{q,1}(t)}{C_{CO_2,1}(t)} = \frac{C_{q,2}(t)}{C_{CO_2,2}(t)} = \dots = P_t \frac{E_q}{E_{CO_2}} \quad (10)$$

Similar as Scenario 1, the infection risk and excess  $CO_2$  threshold can then be derived as:

$$P_i = 1 - e^{-BP_t \frac{E_q}{E_{CO_2}} \int_0^{T_i} C_{CO_2}(t) dt} \quad (11)$$

$$C_t = \frac{E_{CO_2}}{E_q T_i B P_t} \ln \left( \frac{1}{1 - P_t} \right) \quad (12)$$

Equation (11) can be treated as an extension of the classical RF-based infection risk model.

The generality of the original model is extended from scenarios with fixed occupants (scenario

204 1) to scenarios with varying occupancy levels (scenario 2), with initial quanta/excess  $CO_2$  to  
205 be taken into account. It should be noted that  $T_i$  in Scenario 2 is usually hard to monitor as the  
206 occupancy level keeps changing. An alternative method is to predefine it according to the  
207 characteristics of different spaces. For example,  $T_i$  could be set as 35 min for check-in hall and  
208 100 min for departure hall according to the average dwelling times measured in an airport (Mihi  
209 et al., 2018).

### 210 2.2.3 Scenario 3: Non-regularly attended spaces with changing infection ratios

211 In Scenario 3, indoor infection ratio cannot be represented by  $P_i$  due to the relatively low  
212 occupancy level.  $I_i$  is therefore recommended as the maximum value of  $\{1, N_i P_i\}$  to provide a  
213 safe indoor environment (as Scenario 1). In these circumstances, the infection ratio would  
214 change among the occupancy stages and quanta concentration, and it would not be represented  
215 by excess  $CO_2$  concentration:  $C_i$  derivation needs to follow the general calculation process (see  
216 Part 2.1).

217 It should be noted that the general calculation process does not require the field measurement  
218 of ACH but relies on a known occupancy profile including the number of occupants and the  
219 duration of occupancy for all the occupancy stages. Thus, this method may be more suitable  
220 for spaces in Scenario 3 where the occupancy profile of  $N_i$  and  $T_i$  of each occupancy stage can  
221 be monitored simultaneously or obtained before the spaces being occupied such as the rail train  
222 or theatre.

### 223 2.3 Uncertainty analysis and inputs

224 Uncertainty analysis was carried out considering  $E_q$  and  $E_{CO_2}$  have interindividual variation

225 and can vary with gender, age, leading uncertainty to  $C_t$ . The probability density functions  
 226 (PDF) of  $E_q$  for three different activities are from recent research of Buonanno et al. (2020a),  
 227 where they found the quanta emission follows a log10-normal distribution, see Table 1.  $E_{CO_2}$   
 228 was also assumed to be lognormally distributed with a standard deviation equal to 20% of its  
 229 mean (Molina and Jones, 2021). The mean value for the distribution is calculated as the average  
 230 value of  $E_{CO_2}$  of female and male individuals aged 30 to 40 years (the most frequent age cohort)  
 231 with a specific metabolic equivalent (Persily and de Jonge, 2017). The metabolic equivalent  
 232 for  $E_{CO_2}$  is specified by different activity levels, specifically, 1.5 met for sedentary activity, 3  
 233 met for light activity, 9 met for heavy activity (Ainsworth et al., 2000). Latin Hypercube  
 234 sampling (LHS) (Fang et al. 2005) was used to generate a total of 30,000 samples from  
 235 emissions of quanta and  $CO_2$  due to its advantage in reflecting the true underlying distribution  
 236 of inputs with a smaller sample size. Monte Carlo simulations (Sobol', 1994) were used to  
 237 propagate and quantify the uncertainty in predictions.

238 **Table 1. Inputs for Uncertainty Analysis. Distribution mean and standard deviation in brackets**

Activity	Quanta emission PDF (quanta/h)	CO <sub>2</sub> emission PDF (mL/s)
Sedentary - breathing	LN10 (-0.429, 0.720)	LN (5.05, 1.01)
Light activity - speaking	LN10 (0.698, 0.720)	LN (10.10, 2.02)
Heavy activity - breathing	LN10 (0.399, 0.720)	LN (34.20, 6.84)

239 Typical indoor environments were selected for each scenario based on factors such as  
 240 occupancy level, infection ratio etc. (Tables 2 and 3). Cases in Scenario 1 have a fixed but  
 241 different number of occupants considering that this is a dominant parameter in deriving  $C_t$  in  
 242 Scenario 1, see Equation (9). It should be noted that the case of lecture hall in Scenario 1 has 3  
 243 infectors due to its high occupancy level, whereas other cases have only 1 infector due to the

244 relatively low occupancy level. In Scenario 2 a shopping center was taken as case study with  
 245 variable levels of community prevalence, which were adopted from three different COVID-19  
 246 periods in the UK for 2020 (Pouwels et al., 2021) to represent relatively small (0.06%), median  
 247 (0.4%) and high (1%) community prevalence, among which the highest level of community  
 248 prevalence was adopted for Scenario 1 and Scenario 3. Two cases with low and changing  
 249 occupancy levels were selected for Scenario 3 (i.e., train coach and gym room). As regards  
 250 occupancy stages, only one stage was included for cases in Scenario 1 and Scenario 2 whereas  
 251 five occupancy stages were included for cases in Scenario 3 to take into account the variability  
 252 in  $C_t$  due to the impact of initial quanta/excess  $CO_2$ . Different categories of activities were  
 253 considered in the cases of the different scenarios. Cases in Scenario 1 are assumed to have  
 254 “sedentary activity - breathing” typical of people sitting or standing in office or classroom  
 255 environments. Cases in Scenario 2 are assumed to have “light activity - speaking”, considering  
 256 that people are usually walking in the shopping center and talking to each other. For scenario  
 257 3, two activities are included to explore the effects of activity level on  $C_t$  derivation, specifically,  
 258 “sedentary activity – breathing” for the train coach and “moderate activity – breathing” for  
 259 gym. The breathing rates ( $B$ ) corresponding to different physical activity level is adopted are  
 260 from previous research (Adams, 1993).

261 **Table 2. Inputs of uncertainty analysis for Scenario 1 and Scenario 2.**

Case	Volume (m <sup>3</sup> )	Infectior number	Occupant number	Exposure time (h)	Community prevalence	Breathing rate (m <sup>3</sup> /h)
<b>Scenario 1</b>						
Classroom	231	1	30	1	1%	0.54
Lecture classroom	270	1	65	1	1%	0.54
Lecture hall	540	3	300	1	1%	0.54
Open-plan office	594	1	20	1	1%	0.54
<b>Scenario 2</b>						

Shopping center	2040	-	-	1	0.06%, 0.4%, 1%	1.38
-----------------	------	---	---	---	-----------------	------

262 **Table 3. Inputs of uncertainty analysis for Scenario 3**

Scenario 3	Stage 1	Stage 2	Stage 3	Stage 4	Stage 5
<b>Train coach (300 m<sup>3</sup>)</b>					
Infector number	1	1	1	1	1
Occupant number	20	40	80	40	20
Exposure time (h)	1	1	1	1	1
Community prevalence	1%	1%	1%	1%	1%
Breathing rate (m <sup>3</sup> /h)	0.54	0.54	0.54	0.54	0.54
<b>Gym (600 m<sup>3</sup>)</b>					
Infector number	1	1	1	1	1
Occupant number	5	10	20	10	5
Exposure time (h)	1	1	1	1	1
Community prevalence	1%	1%	1%	1%	1%
Breathing rate (m <sup>3</sup> /h)	3.30	3.30	3.30	3.30	3.30

263 **3. Results**264 *3.1 Safety excess CO<sub>2</sub> threshold varies in different scenarios*

265 For Scenario 1, the number of occupants ( $N_i$ ) is the dominant factor governing  $C_t$  that scales  
266 with it (see Equation (9)).  $C_t$  for cases with different  $N_i$  in Scenario 1 (regularly attended spaces)  
267 have substantial differences, see Figure 1(a). The highest  $C_{t50}$  (the median value of  $C_t$ ) occurs  
268 in lecture hall (890 ppm), followed by lecture classroom (580 ppm), classroom (270 ppm), the  
269 lowest one is in office environment (180 ppm), although significant overlaps exist in the output  
270 distributions (Figure 1(a)).

271 For Scenario 2, instead of  $N_i$ ,  $C_t$  is dominated by community prevalence ( $P_I$ ), as  $C_t$  is  
272 inversely proportional to  $P_I$  (see Equation (12)). Three different values of  $P_I$  (i.e., 0.06%, 0.4%  
273 and 1%) are adopted to derive  $C_t$  and the results are showed in Figure 1(b). The highest  $C_{t50}$  of  
274 870 ppm refers to the lowest  $P_I$  of 0.06% and the lowest  $C_{t50}$  of 50 ppm to the highest  $P_I$  of 1%.

275 For Scenario 3, the changing infection ratios lead to different values of  $C_t$  for different

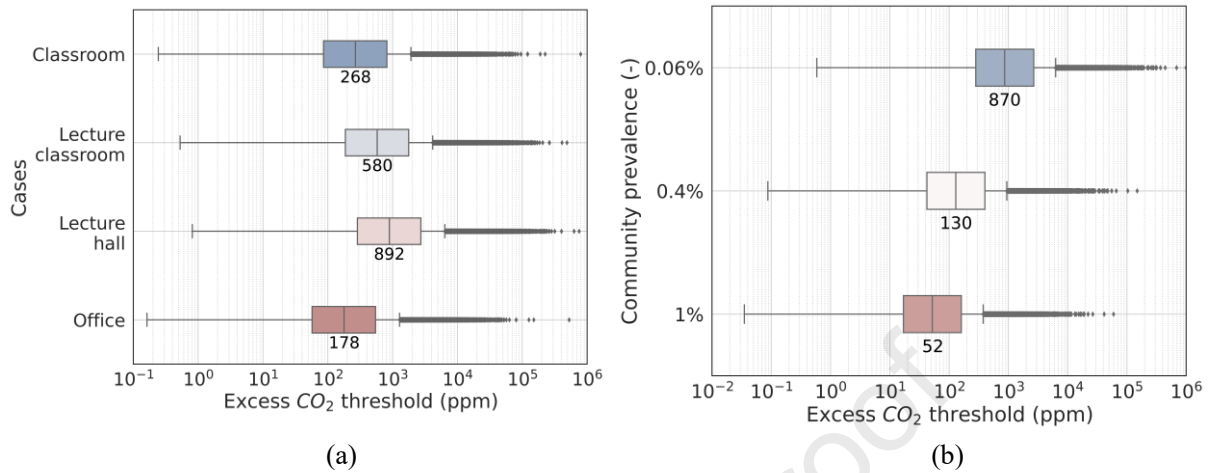
276 occupancy stages. For train coach,  $C_{t50}$  are approx. 180 ppm, 320 ppm, 650 ppm, 410 ppm and  
277 200 ppm corresponding to infection ratios of 1/20, 1/40, 1/80, 1/40 and 1/20 for the five stages  
278 in sequence, while they are 7 ppm, 15 ppm, 30 ppm, 15 ppm and 7 ppm for gym environment  
279 corresponding to infection ratios of 1/5, 1/10, 1/20, 1/10 and 1/5. The changing infection ratios  
280 can lead to different  $C_t$  values in different stages mainly because the existence of initial  
281 quanta/excess  $CO_2$ . For instance, for Stage 2 and Stage 4 of train coach with the same occupant  
282 number of 40,  $C_{t50}$  should be same if initial quanta/excess  $CO_2$  is not considered, but in fact the  
283 difference of  $C_{t50}$  between the two occupancy stages reaches approx. 80 ppm due to the impact  
284 of initial quanta/excess  $CO_2$ .

285 In addition, the general cases in Scenario 3 also proves that activity level is another major  
286 factor which can affect the derived thresholds, see Figure 1(c).  $C_t$  for gym with a high activity  
287 level is much lower than that for train coach with a sedentary activity level due to relative high  
288 activity level in gym environment (hence, high emission rate for quanta). This agrees with  
289 previous studies (Chen et al., 2022; Jia et al., 2022) that there should be much higher restriction  
290 in spaces with high activities such as gym to control airborne infection risk.

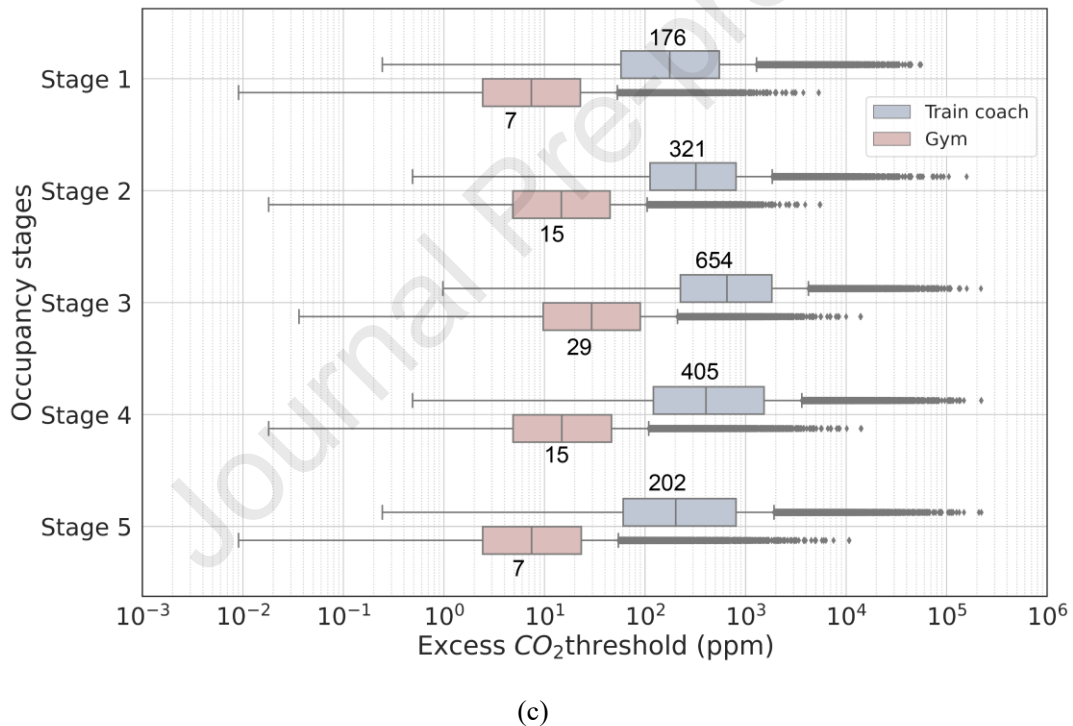
291 Apart from the substantially different  $C_t$  among different cases, large uncertainty of  $C_t$  was  
292 also found in each case, spanning up to six orders of magnitude on a log scale (see Figure 1).  
293 Figure 1 shows that cases with a large median value contain more uncertainty due to a more  
294 right-shifted log-scaled distribution of  $C_t$ , indicating that  $C_t$  can be more affected by the  
295 uncertainty of emission settings considered in our study. Considering the large uncertainty of  
296  $C_t$  and the non-normal distribution when transformed to a linear scale, the median safe excess  
297  $CO_2$  threshold ( $C_{t50}$ ) is an appropriate descriptive statistic for excess  $CO_2$  threshold due to its

298 high probability density (see the violin plot in Figure 1) (Jones et al., 2021).

299



300



301

302

303 **Figure 1.** Safe excess CO<sub>2</sub> thresholds for 3 scenarios: (a) Scenario 1 (with fixed occupancy);

304 (b) Scenario 2 (with changing occupancy but fixed infection ratios); (c) Scenario 3 (with

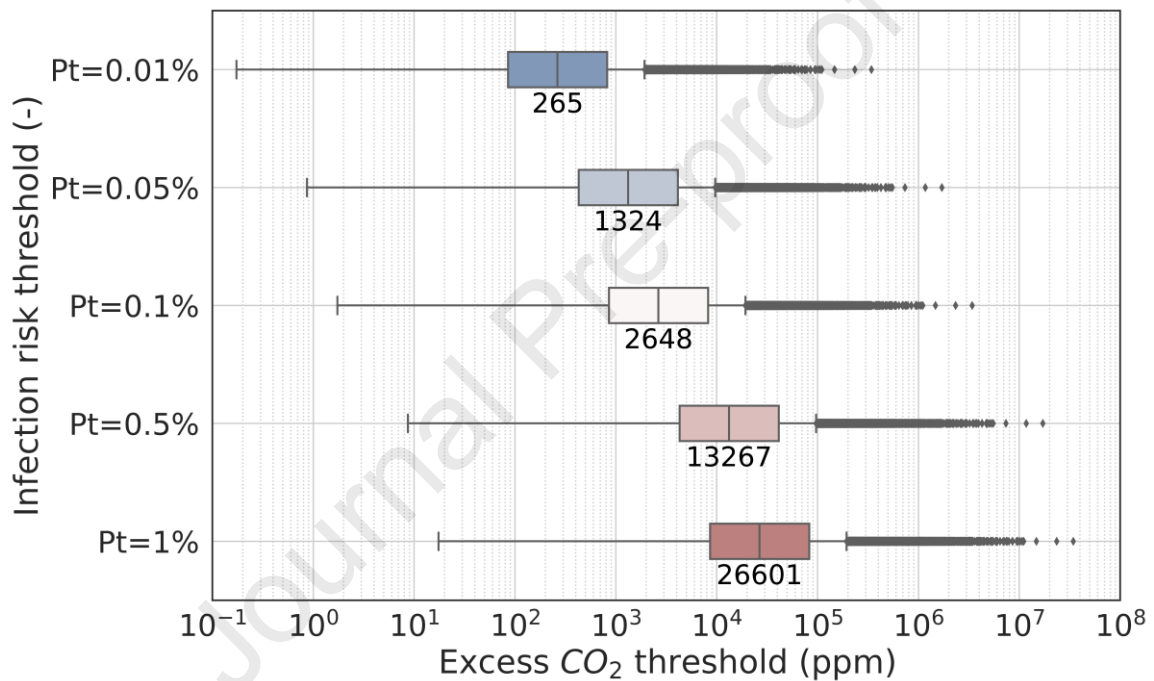
305 changing occupancy and non-fixed infection ratios).

306 3.2 Effect of infection risk threshold ( $P_t$ )

307 As discussed before, the infection risk threshold ( $P_t$ ) plays a role in deriving  $C_t$ . Different  $P_t$

308 have been adopted in different research in the range of 0.01% to 1% (Buonanno et al., 2020b;  
 309 Dai and Zhao, 2020; Peng and Jimenez, 2021; Zhang et al., 2021). Here we explore how  $P_t$  will  
 310 affect  $C_t$  with results shown in Figure 2. The base case is the classroom in Scenario 1 (see Table  
 311 2).  $C_{t50}$  is found to be approximately linearly related to  $P_t$  with approx. 270 ppm for  $P_t = 0.01\%$   
 312 to 27000 ppm for  $P_t = 1\%$ , which reveals the high sensitivity of  $C_{t50}$  to  $P_t$ .

313



314 **Figure 2.** Excess  $CO_2$  thresholds for the classroom (see Table 2) under different infection risk  
 315 thresholds.

### 316 3.3 Effect of Initial Conditions

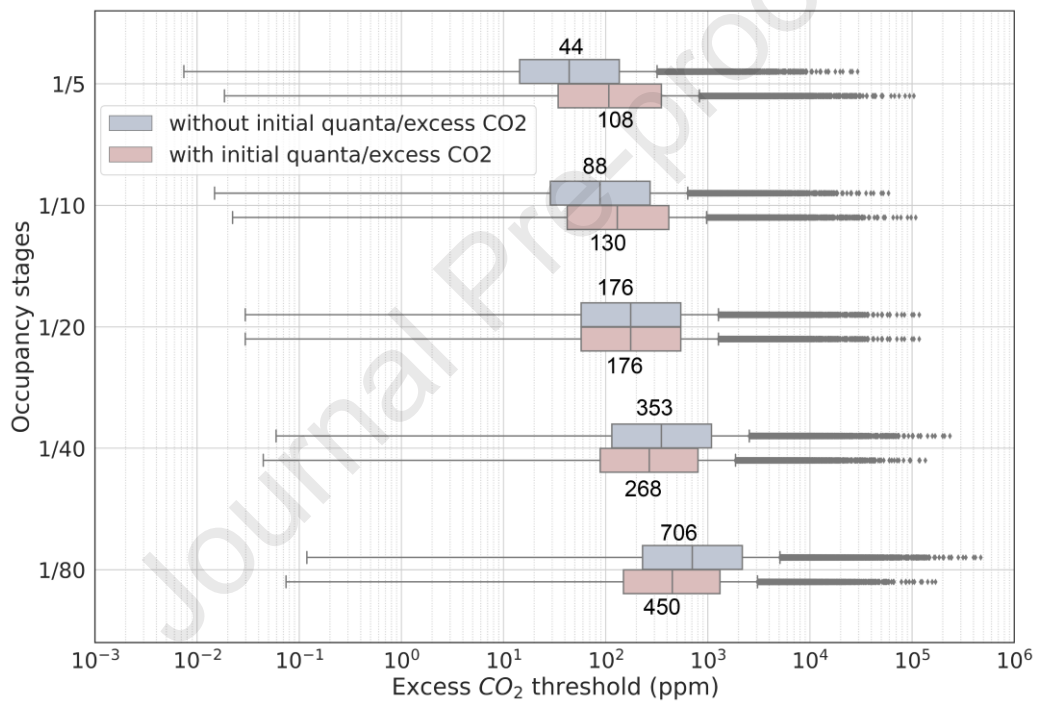
317 We have shown that initial condition of quanta and excess  $CO_2$  can affect the derived safe  
 318 excess  $CO_2$  threshold when infection ratio varies among the occupancy stages. However, most  
 319 previous studies overlook the initial condition of quanta and excess  $CO_2$  in  $C_t$  derivation (Hou  
 320 et al., 2021; Peng and Jimenez, 2021; Rudnick and Milton, 2003). To further quantify the

321 impact of initial condition of quanta/excess  $CO_2$  on  $C_t$  when infection ratio varies, we compare  
322 two cases: 1) considering the initial condition of quanta/excess  $CO_2$ ; 2) no initial quanta/excess  
323  $CO_2$ . We consider two cases with the same indoor volume of  $300\text{ m}^3$ , being occupied both with  
324 two stages. The occupants in the two cases are assumed to have “sedentary activity – breathing”,  
325 and only 1 infector is adopted.

326 Case 1 assumes there are 20 occupants in Stage 1, and the occupant number in Stage 2  
327 changes to 5, 10, 20, 40, 80 respectively, which means the infection ratio will change from  $1/20$   
328 (Stage 1) to  $1/5$ ,  $1/10$ ,  $1/20$ ,  $1/40$ ,  $1/80$  (Stage 2) accordingly and initial quanta/excess  $CO_2$  can  
329 affect  $C_t$  in Stage 2 in varying degrees. Case 2 assumes there are no occupants in Stage 1 (hence  
330 no initial quanta/excess  $CO_2$ ), and 5 different occupancy levels are assumed for Stage 2 just  
331 like case 1. Here we aim to derive  $C_t$  for Stage 2 for both two cases with consideration of the  
332 impacts of initial quanta/excess  $CO_2$  from Stage 1 (case 1) and without (case 2). The differences  
333 of results between the two cases can be used to quantify the impact of initial quanta/excess  $CO_2$   
334 on  $C_t$ . It's easy to derive  $C_t$  for case 2 as there are no initial quanta/excess  $CO_2$ , while for case  
335 1, an estimation of initial quanta/excess  $CO_2$  released from stage 1 is needed. Considering the  
336 excess  $CO_2$  concentration is affected by different factors such as exposure time and ACH during  
337 Stage 1, here we assumed a constant value for initial excess  $CO_2$  concentration for Stage 2 in  
338 case 1, namely, 1000 ppm. Initial quanta can then be derived based on it and infection ratios of  
339 Stage 1 (see Eq. S4 in Supplementary).

340 Figure 3 shows there are distinct differences of derived  $C_t$  between the cases with and  
341 without considering initial quanta/excess  $CO_2$  when infection ratio of Stage 2 differs from  
342 Stage 1 ( $1/20$ ), suggesting the initial condition of quanta/excess  $CO_2$  shouldn't be ignored in

343  $C_t$  derivation. Overall, when infection ratio increases (larger than 1/20) from Stage 1,  $C_t$   
 344 considering initial condition is larger than that without considering initial quanta/excess  $CO_2$ ,  
 345 and vice versa. The difference will be higher when the infection ratio deviates more from the  
 346 base case of 1/20. When the infection ratio increases from 1/20 (Stage 1) to 1/5 (Stage 2),  $C_{t50}$   
 347 increases by 60 ppm than that without considering initial quanta/excess  $CO_2$  and when the  
 348 Stage 2 infection ratio decreases from 1/20 to 1/80,  $C_{t50}$  becomes 260 ppm lower.  
 349



350 **Figure 3.** Excess  $CO_2$  threshold of the second occupancy stage of an indoor space ( $300\text{ m}^3$ )  
 351 under different infection ratios considering with and without initial quanta/ $CO_2$

## 352 4. Discussion

### 353 4.1. New understanding of rebreathed-fraction model

354 RF-based Wells-Riley model proposed by Rudnick and Milton's (2003) used  $CO_2$  as a marker

355 for exhaled-breath exposure and avoided ACH estimation for airborne infection risk  
356 assessment. The model does not require any knowledge about ACH, hence it has been widely  
357 used in assessing airborne infection risk (Andrews et al., 2014; Hella et al., 2017; Richardson  
358 et al., 2014; Wood et al., 2014; Zürcher et al., 2020). However, However, we proved that RF-  
359 based model should be only adopted for spaces with fixed occupancy otherwise initial quanta  
360 will cause bias of it (see Part 3.3), but this is largely overlooked by many other studies. For  
361 spaces with varying occupancy, the initial quanta/excess  $CO_2$  generated by previous occupants  
362 but remaining in the air can be very important determining the overall quanta/excess  $CO_2$   
363 concentration for next-stage occupancy. How will RF-based model deal with initial  
364 quanta/excess  $CO_2$  for spaces with changing occupancy has not been adequately discussed  
365 before. In this article, we made analytical derivation to explain the mechanism of RF-based  
366 method in dealing with initial quanta/excess  $CO_2$ . We showed that initial quanta/excess  $CO_2$   
367 can be considered within the RF-based method in  $C_t$  derivation for Scenario 1 (with fixed  
368 occupancy) and Scenario 2 (with changing occupancy but fixed infection ratios). This further  
369 extends the generalization of RF-based model from spaces with fixed occupancy to spaces with  
370 changing occupancy. It should be noted that other recent studies (Burridge et al., 2021; Vouriot  
371 et al., 2021) resonate with our study in that they apply RF-based model to spaces with varying  
372 occupancy levels to assess infection risk. However, only two occupancy modes were  
373 considered in these studies, occupied and non-occupied, which are both included in our  
374 Scenario 1. In this contribution, we have proved that for spaces with both occupied and non-  
375 occupied modes, the non-occupied period does not affect the proportion of quanta  
376 concentration to excess  $CO_2$  concentration in future occupied period if infection ratios remain

377 unchanged given only ventilation is considered here (see Supplementary Information).

#### 378 4.2. Implications for $C_t$ determination

379 Great uncertainty in  $C_t$  can be caused by the uncertainty of emissions ( $E_q$  and  $E_{CO_2}$ ) (see  
380 Figure 1).  $E_{CO_2}$  and  $E_q$  contain uncertainty because they have interindividual variation and can  
381 be affected by factors such as age, gender (Buonanno et al., 2020a; Persily and de Jonge, 2017;  
382 Good et al., 2021). The value of  $E_q$  can vary by up to 3 orders of magnitude (e.g., 0.32-240  
383 quanta/h for speaking under light activity) (Buonanno et al., 2020a) while  $E_{CO_2}$  varies within  
384 only one order of magnitude (e.g., 2.88-43.2 L/h) (Persily and de Jonge, 2017). Different  
385 studies adopted very different values of  $E_q$  and therefore could lead to very different  $C_t$ . For  
386 only the classroom settings with the same activity level, the median value of  $E_q$  in our study is  
387 0.37 quanta/h (Buonanno et al., 2020a), while it was in the range of 27.55 quanta/h to 100  
388 quanta/h in other studies (Bazant et al., 2021; Hou et al., 2021; Peng and Jimenez, 2021),  
389 resulting in several hundred times lower  $C_t$  than our results.

390 The choice of  $P_t$  and  $I_t$  have also an impact  $C_t$ . Theoretically, lower  $P_t$  can promise safer  
391 indoor environment, but this would come at the cost of very low  $C_t$  practically impossible to  
392 achieve in real-world scenarios. E.g., a low level of  $C_t$  may require a very high ACH, unfeasible  
393 and prone to cause large energy cost due to the diminishing return phenomenon of ventilation  
394 (Li et al., 2021). Besides, how to determine the infector number  $I_t$  is also important as it is  
395 related to the total quanta emission. Our study defined  $I_t$  to be the maximum value of  $\{1, P_t N_i\}$   
396 as the worst-case scenario. On the contrary, Bazant et al. (2021) considered  $I_t$  to be the  
397 minimum value of  $\{1, P_t N_i\}$ , which resulted in a dramatically large  $C_t$  (even larger than 10000

398 ppm) when  $P_I$  is small.

#### 399 4.3. Implications for infection risk monitoring and control

400 Our model has practical significance for indoor transmission monitoring and control. For  
401 Scenario 1 and Scenario 2, safe excess  $CO_2$  threshold is related to variables such as occupancy  
402 level, duration and risk threshold through simple equations (see Equation (9) and Equation  
403 (12)), making it possible to apply our model for infection risk monitoring in Scenario 1 and 2  
404 for public individuals. For instance, when arriving at a space such as a shopping center (as our  
405 Scenario 2), people can easily measure the indoor excess  $CO_2$  level first through a portable  
406 low-cost  $CO_2$  sensor, then by replacing  $C_I$  in Equation (12) by the measured data, people can  
407 roughly obtain a safe exposure duration for that shopping center based on their acceptable risk  
408 threshold to guide how long they should stay in the shopping center. Furthermore, taking into  
409 account the impact of initial quanta/excess  $CO_2$  on risk estimation and  $C_I$  derivation, our model  
410 can be adopted to further develop different ventilation control strategies such as  $CO_2$ -based  
411 demand-controlled ventilation (Li and Cai, 2022) or intermittent ventilation strategy (Melikov  
412 et al., 2020; Zhang et al., 2022) with an objective to reduce indoor transmission risk by treating  
413 indoor excess  $CO_2$  as a control variable.

414 Further applying our calculation framework into real-world scenarios, some insights can be  
415 gained by comparing derived  $C_I$  with measurement data/standard limits. For Scenario 1, the  
416 occupant numbers can largely affect  $C_I$  level, thus, it's warranted to concurrently consider  $CO_2$   
417 level and occupant level in transmission risk evaluation of an indoor environment. For example,  
418 for classrooms in Scenario 1, the measured excess  $CO_2$  level was found to be in the range of

419 300 - 2500 ppm (outdoor level of 420 ppm) dependent on the number of occupants (Bakó-Biró  
420 et al., 2012; Vouriot et al., 2021; Persily et al., 2022). According to our framework, 300 ppm  
421 can represent an unsafe environment if the occupant number is less than 33, and 2500 ppm can  
422 still be a safe level if occupants is larger than 278. Therefore,  $C_t$  threshold should be used in  
423 conjunction with occupant number. For scenario 2, community prevalence can dominate  $C_t$  and  
424 can be used as a reference for lockdown policy implementation. It was found that the one-hour  
425 average  $CO_2$  level of 40% shopping mall in Hong Kong exceeded 1000 ppm (Li et al., 2001).  
426 To keep infection risk no more than 0.01% for shopping malls, a community prevalence of less  
427 than 0.09% is needed according to our calculation framework, otherwise, such places should  
428 be locked down. For Scenario 3, taking a restaurant ( $\sim 350 \text{ m}^3$ ) for example, considering two  
429 occupancy stage ( $N_1 = 20$  for Stage 1 and  $N_2 = 80$  for Stage 2) (Shen et al., 2021), according to  
430 ASHRAE 62.1 (ASHRAE, 2019), the maximum excess  $CO_2$  limits (the steady-state excess  
431  $CO_2$  concentration under the required ventilation rate) for the first two occupancy stages are  
432 540 ppm (Stage 1) and 790 ppm (Stage 2) respectively. But  $C_t$  calculated from our framework  
433 amounts to 180 ppm and 610 ppm, respectively. The difference indicates the target of infection  
434 risk control should be integrated into present ventilation standards to promise both a high level  
435 of IAQ and a low infection risk.

#### 436 4.4. Limitation of the study

437 Our study is based on the assumption that outdoor ventilation is the only loss mechanism  
438 for quanta in Scenario 1 and Scenario 2, which results in a constant proportion between quanta  
439 concentration and excess  $CO_2$  concentration, hence making RF-based model suitable for

440 deriving  $C_t$  for Scenario 1 and 2. However, surface deposition, filtration and virus deactivation  
441 could significantly contribute to reduce quanta concentration (Blocken et al., 2021; Su et al.,  
442 2021; van Doremalen et al., 2020). Neglecting these loss mechanisms may overestimate indoor  
443 quanta concentration and result in a lower estimate of  $C_t$  than needed. However, the reliability  
444 of the derived  $C_t$  for a safe indoor environment would not be affected.

445 The thresholds we derived are based on the assumption of a well-mixed room air. Thus, the  
446 location of  $CO_2$  sensors needs to be carefully selected to adequately reflect indoor  $CO_2$   
447 conditions (Mahyuddin and Awbi, 2010; Mahyuddin et al., 2014). Additionally, our results only  
448 account for long-range airborne transmission neglecting the contribution of short-range  
449 transmission (Chen et al., 2021; Gao et al., 2021; Li, 2021). Limiting to monitoring infection  
450 risk based on  $C_t$  values may not be sufficient. Other intervention measures such as wearing  
451 masks and social distancing should be jointly considered to control indoor airborne  
452 transmission (Jarvis, 2020; Mittal et al., 2020a; Wagner et al., 2021).

453 Another limitation lies in the application of community prevalence ( $P_I$ ) in our study. For  
454 scenario 1 and scenario 3,  $P_I$  is used to determine the indoor infector number, which would  
455 cause bias because 1)  $P_I$  might be smaller than the real value due to the asymptomatic  
456 characteristic of SARS-CoV-2 (Lee et al., 2020; Pollock and Lancaster, 2020); and 2) positive  
457 individuals may not be present at public spaces due to mandatory quarantine policy which  
458 would lead to a lower indoor infection ratio than  $P_I$ . For scenario 2, simply using  $P_I$  to represent  
459 the indoor infection ratio can lead to underestimate the real indoor infection ratio when the  
460 number of occupants is small. Conducting field measurement to estimate the average

461 occupancy level ( $N_{ave}$ ) and selecting the maximum value of  $\{1, N_{ave}P_I\}$  could be an alternative  
462 method for defining a convincing infection ratio for scenario 2. In addition, considering  $P_I$  is  
463 changing during different time periods of pandemic, the indoor infection ratio would need to  
464 be updated accordingly.

465 In addition, the uncertainty of  $C_t$  estimated by our study may be limited as we only  
466 considered the uncertainty in emission settings (i.e., quanta emission rate,  $CO_2$  emission rate)  
467 in  $C_t$  derivation. Community prevalence  $P_I$  may contain uncertainty due to the reasons  
468 mentioned above. The uncertainty of it may increase the uncertainty of  $C_t$  for Scenario 2 where  
469  $P_I$  is a dominating input in  $C_t$  derivation, but it may not obviously affect  $C_t$  for Scenario 1 and  
470 3 because  $P_I$  is adopted in  $C_t$  derivation only when  $P_I N_i > 1$  but the occupancy level ( $N_i$ ) of  
471 most cases in Scenario 1 and 3 is usually low and hence  $P_I N_i < 1$ . Similar as emission settings,  
472 breathing rate can also contain uncertainty due to interindividual differences and factors such  
473 as age and gender. In addition, quanta emission rate,  $CO_2$  emission rate and breathing rate may  
474 all be correlated to each other (Good et al., 2021). In our study, we simply adopted constant  
475 breathing rates for different physical activity levels following the study of Buonanno et al.  
476 (2020a) which estimated the quanta emission rate under different physical activity levels.  
477 Quanta emission rate and  $CO_2$  emission rate are also inter-related through physical activity  
478 level (See Table 1). In future, based on more accurate data, the uncertainty and correlation of  
479 those parameters may be further interpreted, and the uncertainty of  $C_t$  can be therefore further  
480 estimated.

## 481 **5. Conclusion**

482 A new calculation framework was proposed in this study for deriving safe excess  $CO_2$   
483 threshold ( $C_t$ ) for different spaces with consideration of initial quanta/excess  $CO_2$  and  
484 fixed/changing occupancy levels. From our derivation process we found that the proportion of  
485 indoor excess  $CO_2$  concentration to quanta concentration is constant for a constant infection  
486 ratio (infectors/occupants) of an indoor space. Based on this relationship, RF-based (rebreathed  
487 fraction-based) model can be directly applied for infection risk assessment and  $C_t$  derivation  
488 when infection ratio is constant, but not applicable for the cases with varying infection ratios.

489 Affected by factors such as occupant number ( $N_i$ ), community prevalence ( $P_I$ ) and activity  
490 level, the median value  $C_{150}$  derived by our framework varies significantly among the selected  
491 cases, with a minimum value of 7 ppm for gym to a maximum value of 890 ppm for lecture  
492 hall, with long-tailed distributions. Initial quanta/excess  $CO_2$  is found to largely affect  $C_t$   
493 especially when the infection ratio varies significantly among the occupancy stages. A bias of  
494 several hundred ppm (e.g., 260 ppm for a space of 300 m<sup>3</sup> and with sedentary activity level)  
495 could be made if the initial quanta in  $C_t$  derivation is not well considered. Our finding illustrates  
496 that different  $CO_2$  thresholds should be derived for different spaces and different occupancy  
497 stages, rather than being fixed at a constant value for all spaces.

498 Large uncertainty was also found in derived thresholds for all cases, spanning approximately  
499 6 orders of magnitude, which are mainly influenced by quanta emission rate ( $E_q$ ) and  $CO_2$   
500 emission rate ( $E_{CO_2}$ ). For a better control of indoor infection risk through  $CO_2$  monitoring, more  
501 accurate input parameters would be needed.

## 502 **Acknowledgement**

503 XL acknowledged the financial support from China Scholarship Council (CSC) for pursuing  
 504 her PhD at the University of Reading, UK.

## 505 **References**

- 506 Adams, W.C., 1993. Measurement of Breathing Rate and Volume in Routinely Performed Daily  
 507 Activities. Final Report. Human Performance Laboratory, Physical Education Department,  
 508 University of California, Davis. Human Performance Laboratory, Physical Education  
 509 Department, University of California, Davis. Prepared for the California Air Resources  
 510 Board, Contract No. A033-205, April 1993.
- 511 Ainsworth, B.E., Haskell, W.L., Whitt, M.C., Irwin, M.L., Swartz, A.M., Strath, S.J., O'Brien,  
 512 W.L., Bassett, J., Schmitz, K.H., Emplainscourt, P.O., Jacobs, J., Leon, A.S., 2000.  
 513 Compendium of physical activities: An update of activity codes and MET intensities. *Med  
 514 Sci Sports Exerc* 32. <https://doi.org/10.1097/00005768-200009001-00009>
- 515 Andrews, J.R., Morrow, C., Walensky, R.P., Wood, R., 2014. Integrating social contact and  
 516 environmental data in evaluating tuberculosis transmission in a South African township.  
 517 *Journal of Infectious Diseases* 210, 597–603. <https://doi.org/10.1093/infdis/jiu138>
- 518 ASHRAE, 2019. ANSI/ASHRAE Standard 62.1-2019, Ventilation for acceptable indoor  
 519 airquality. Peachtree Corners, GA: ASHRAE.
- 520 Bakó-Biró, Z., Clements-Croome, D.J., Kochhar, N., Awbi, H.B., Williams, M.J., 2012.  
 521 Ventilation rates in schools and pupils' performance. *Build Environ* 48, 215–223.  
 522 <https://doi.org/10.1016/j.buildenv.2011.08.018>
- 523 Bazant, M.Z., Kodio, O., Cohen, A.E., Khan, K., Gu, Z., Bush, J.W.M., 2021. Monitoring  
 524 carbon dioxide to quantify the risk of indoor airborne transmission of COVID-19. *Flow* 1,  
 525 1–17. <https://doi.org/10.1017/flo.2021.10>
- 526 Blocken, B., van Druenen, T., Ricci, A., Kang, L., van Hooff, T., Qin, P., Xia, L., Ruiz, C.A.,  
 527 Arts, J.H., Diepens, J.F.L., Maas, G.A., Gillmeier, S.G., Vos, S.B., Brombacher, A.C.,  
 528 2021. Ventilation and air cleaning to limit aerosol particle concentrations in a gym during  
 529 the COVID-19 pandemic. *Building and Environment* 193, 107659.  
 530 <https://doi.org/10.1016/j.buildenv.2021.107659>
- 531 Buonanno, G., Morawska, L., Stabile, L., 2020a. Quantitative assessment of the risk of airborne  
 532 transmission of SARS-CoV-2 infection: Prospective and retrospective applications.  
 533 *Environ Int* 145, 106112. <https://doi.org/10.1016/j.envint.2020.106112>
- 534 Buonanno, G., Stabile, L., Morawska, L., 2020b. Estimation of airborne viral emission : Quanta  
 535 emission rate of SARS-CoV-2 for infection risk assessment. *Environ Int* 141, 105794.  
 536 <https://doi.org/10.1016/j.envint.2020.105794>
- 537 Burridge, H.C., Fan, S., Jones, R.L., Noakes, C.J., Linden, P.F., 2021. Predictive and  
 538 retrospective modelling of airborne infection risk using monitored carbon dioxide. *Indoor  
 539 and Built Environment* 1420326X2110435. <https://doi.org/10.1177/1420326x211043564>
- 540 CDC, 2021. Ventilation in buildings. Atlanta: Centers for Disease Control and Prevention.  
 541 <https://www.cdc.gov/coronavirus/2019-ncov/community/ventilation.html>
- 542 Chen, N., Zhou, M., Dong, X., Qu, J., Gong, F., Han, Y., Qiu, Y., Wang, J., Liu, Y., Wei, Y., Xia,  
 543 J., Yu, T., Zhang, X., Zhang, L., 2020. Epidemiological and clinical characteristics of 99

- 544 cases of 2019 novel coronavirus pneumonia in Wuhan, China: a descriptive study. *The*  
545 *Lancet* 395, 507–513. [https://doi.org/10.1016/S0140-6736\(20\)30211-7](https://doi.org/10.1016/S0140-6736(20)30211-7)
- 546 Chen, W., Qian, H., Zhang, N., Liu, F., Liu, L., Li, Y., 2022. Extended short-range airborne  
547 transmission of respiratory infections. *J Hazard Mater* 422.  
548 <https://doi.org/10.1016/j.jhazmat.2021.126837>
- 549 CIBSE, C., 2020. COVID-19 Ventilation Guidance. [https://www.cibse.org/Coronavirus-](https://www.cibse.org/Coronavirus-COVID-19)  
550 [COVID-19](https://www.cibse.org/Coronavirus-COVID-19)
- 551 Dai, H., Zhao, B., 2020. Association of the infection probability of COVID-19 with ventilation  
552 rates in confined spaces. *Build Simul* 13, 1321–1327. [https://doi.org/10.1007/s12273-](https://doi.org/10.1007/s12273-020-0703-5)  
553 [020-0703-5](https://doi.org/10.1007/s12273-020-0703-5)
- 554 EMG/SPI-B, 2021. Application of CO2 monitoring as an approach to managing ventilation to  
555 mitigate SARS-CoV-2 transmission. [https://www.gov.uk/government/publications/emg-](https://www.gov.uk/government/publications/emg-and-spi-b-application-of-co2-monitoring-as-an-approach-to-managing-ventilation-to-mitigate-sars-cov-2-transmission-27-may-2021)  
556 [and-spi-b-application-of-co2-monitoring-as-an-approach-to-managing-ventilation-to-](https://www.gov.uk/government/publications/emg-and-spi-b-application-of-co2-monitoring-as-an-approach-to-managing-ventilation-to-mitigate-sars-cov-2-transmission-27-may-2021)  
557 [mitigate-sars-cov-2-transmission-27-may-2021](https://www.gov.uk/government/publications/emg-and-spi-b-application-of-co2-monitoring-as-an-approach-to-managing-ventilation-to-mitigate-sars-cov-2-transmission-27-may-2021)
- 558 Fang, K.-T., Li, R., Sudjianto, A., 2005. Design and Modeling for Computer Experiments (1st  
559 ed.). Chapman and Hall/CRC. <https://doi.org/10.1201/9781420034899>
- 560 Furuya, H., Nagamine, M., Watanabe, T., 2009. Use of a mathematical model to estimate  
561 tuberculosis transmission risk in an Internet café. *Environ Health Prev Med* 14, 96–102.  
562 <https://doi.org/10.1007/s12199-008-0062-9>
- 563 Gao, C.X., Li, Y., Wei, J., Cotton, S., Hamilton, M., Wang, L., Cowling, B.J., 2021. Multi-route  
564 respiratory infection: When a transmission route may dominate. *Science of the Total*  
565 *Environment* 752, 141856. <https://doi.org/10.1016/j.scitotenv.2020.141856>
- 566 Gammaitoni, L., Nucci, M. C., 1997. Using a mathematical model to evaluate the efficacy of  
567 TB control measures. *Emerging infectious diseases*, 3(3), 335–342.  
568 <https://doi.org/10.3201/eid0303.970310>
- 569 Good, N., Fedak, K.M., Goble, D., Keisling, A., L'Orange, C., Morton, E., Phillips, R., Tanner,  
570 K., Volckens, J., 2021. Respiratory Aerosol Emissions from Vocalization: Age and Sex  
571 Differences Are Explained by Volume and Exhaled CO2. *Environ Sci Technol Lett* 8,  
572 1071–1076. <https://doi.org/10.1021/acs.estlett.1c00760>
- 573 Hella, J., Morrow, C., Mhimbira, F., Ginsberg, S., Chitnis, N., Gagneux, S., Mutayoba, B.,  
574 Wood, R., Fenner, L., 2017. Tuberculosis transmission in public locations in Tanzania: A  
575 novel approach to studying airborne disease transmission. *Journal of Infection* 75, 191–  
576 197. <https://doi.org/10.1016/j.jinf.2017.06.009>
- 577 Hou, D., Katal, A., Wang, L. (Leon), Katal, A., Wang, L. (Leon), 2021. Bayesian Calibration  
578 of Using CO2 Sensors to Assess Ventilation Conditions and Associated COVID-19  
579 Airborne Aerosol Transmission Risk in Schools. *medRxiv* 2021.01.29.21250791.
- 580 Jarvis, M.C., 2020. Aerosol Transmission of SARS-CoV-2: Physical Principles and  
581 Implications. *Front Public Health*. <https://doi.org/10.3389/fpubh.2020.590041>
- 582 Jia, W., Wei, J., Cheng, P., Wang, Q., Li, Y., 2022. Exposure and respiratory infection risk via  
583 the short-range airborne route. *Build Environ* 219.  
584 <https://doi.org/10.1016/j.buildenv.2022.109166>
- 585 Jones, B., Sharpe, P., Iddon, C., Hathway, E.A., Noakes, C.J., Fitzgerald, S., 2021. Modelling  
586 uncertainty in the relative risk of exposure to the SARS-CoV-2 virus by airborne aerosol  
587 transmission in well mixed indoor air. *Build Environ* 191.

- 588 <https://doi.org/10.1016/j.buildenv.2021.107617>
- 589 Ke, R., Zitzmann, C., Ho, D. D., Ribeiro, R. M., and Perelson, A. S.: In vivo kinetics of SARS-  
590 CoV-2 infection and its relationship with a person's infectiousness, *Proc. Natl. Acad. Sci.*  
591 U. S. A., 118, <https://doi.org/10.1073/pnas.2111477118>, 2021.
- 592 Ke, R., Martinez, P. P., Smith, R. L., Gibson, L. L., Mirza, A., Conte, M., Gallagher, N., Luo,  
593 C. H., Jarrett, J., Zhou, R., Conte, A., Liu, T., Farjo, M., Walden, K. K. O., Rendon, G.,  
594 Fields, C. J., Wang, L., Fredrickson, R., Edmonson, D. C., Baughman, M. E., Chiu, K. K.,  
595 Choi, H., Scardina, K. R., Bradley, S., Gloss, S. L., Reinhart, C., Yedetore, J., Quicksall,  
596 J., Owens, A. N., Broach, J., Barton, B., Lazar, P., Heetderks, W. J., Robinson, M. L.,  
597 Mostafa, H. H., Manabe, Y. C., Pekosz, A., McManus, D. D., and Brooke, C. B.: Daily  
598 longitudinal sampling of SARS-CoV-2 infection reveals substantial heterogeneity in  
599 infectiousness, *Nat Microbiol*, 7, 640-652, 2022.
- 600 Li, B., Cai, W., 2022. A novel CO<sub>2</sub>-based demand-controlled ventilation strategy to limit the  
601 spread of COVID-19 in the indoor environment. *Build Environ* 219.  
602 <https://doi.org/10.1016/j.buildenv.2022.109232>
- 603 Lee, S., Kim, T., Lee, E., Lee, C., Kim, H., Rhee, H., Park, S.Y., Son, H.J., Yu, S., Park, J.W.,  
604 Choo, E.J., Park, S., Loeb, M., Kim, T.H., 2020. Clinical Course and Molecular Viral  
605 Shedding among Asymptomatic and Symptomatic Patients with SARS-CoV-2 Infection  
606 in a Community Treatment Center in the Republic of Korea. *JAMA Intern Med* 180,  
607 1447–1452. <https://doi.org/10.1001/jamainternmed.2020.3862>
- 608 Lelieveld, J., Helleis, F., Borrmann, S., Cheng, Y., Drewnick, F., Haug, G., Klimach, T., Sciare,  
609 J., Su, H., Pöschl, U., 2020. Model calculations of aerosol transmission and infection risk  
610 of covid-19 in indoor environments. *Int J Environ Res Public Health* 17, 1–18.  
611 <https://doi.org/10.3390/ijerph17218114>
- 612 Li, W.M., Lee, S.C., Chan, L.Y., 2001. Indoor air quality at nine shopping malls in Hong Kong.  
613 *Science of The Total Environment* 273, 27–40. [https://doi.org/10.1016/S0048-](https://doi.org/10.1016/S0048-9697(00)00833-0)  
614 [9697\(00\)00833-0](https://doi.org/10.1016/S0048-9697(00)00833-0)
- 615 Li, Y., 2021. Basic routes of transmission of respiratory pathogens—A new proposal for  
616 transmission categorization based on respiratory spray, inhalation, and touch. *Indoor Air*.  
617 <https://doi.org/10.1111/ina.12786>
- 618 Li, Y., Cheng, P., Jia, W., 2021. Poor ventilation worsens short-range airborne transmission of  
619 respiratory infection. *Indoor Air*. <https://doi.org/10.1111/ina.12946>
- 620 Ma, Y., Horsburgh, C.R., White, L.F., Jenkins, H.E., 2018. Quantifying TB transmission: A  
621 systematic review of reproduction number and serial interval estimates for tuberculosis.  
622 *Epidemiol Infect* 146, 1478–1494. <https://doi.org/10.1017/S0950268818001760>
- 623 Mahyuddin, N., Awbi, H., 2010. The spatial distribution of carbon dioxide in an environmental  
624 test chamber. *Build Environ* 45, 1993–2001.  
625 <https://doi.org/10.1016/j.buildenv.2010.02.001>
- 626 Mahyuddin, N., Awbi, H.B., Alshitawi, M., 2014. The spatial distribution of carbon dioxide in  
627 rooms with particular application to classrooms. *Indoor and Built Environment* 23, 433–  
628 448. <https://doi.org/10.1177/1420326X13512142>
- 629 Melikov, A.K., Ai, Z.T., Markov, D.G., 2020. Intermittent occupancy combined with  
630 ventilation: An efficient strategy for the reduction of airborne transmission indoors.

- 631 Science of the Total Environment 744. <https://doi.org/10.1016/j.scitotenv.2020.140908>
- 632 Mihi, Mirela, Ani, I.-D., Mihi, M, Professor, F., Ani, I., Kursan Milaković, I., Professor, A.,  
633 2018. Time spent shopping and consumer clothing purchasing behaviour EKONOMSKI  
634 PREGLED.
- 635 Miller, S.L., Nazaroff, W.W., Jimenez, J.L., Boerstra, A., Buonanno, G., Dancer, S.J., Kurnitski,  
636 J., Marr, L.C., Morawska, L., Noakes, C., 2021. Transmission of SARS-CoV-2 by  
637 inhalation of respiratory aerosol in the Skagit Valley Chorale superspreading event. *Indoor*  
638 *Air* 31, 314–323. <https://doi.org/10.1111/ina.12751>
- 639 Mittal, R., Meneveau, C., Wu, W., 2020a. A mathematical framework for estimating risk of  
640 airborne transmission of COVID-19 with application to face mask use and social  
641 distancing. *Physics of Fluids* 32. <https://doi.org/10.1063/5.0025476>
- 642 Mittal, R., Ni, R., Seo, J.H., 2020b. The flow physics of COVID-19. *J Fluid Mech* 894.  
643 <https://doi.org/10.1017/jfm.2020.330>
- 644 Molina, C., Jones, B., 2021. Investigating Uncertainty in the Relationship between Indoor  
645 Steady-State CO<sub>2</sub> Concentrations and Ventilation Rates. *Airc.*  
646 <https://doi.org/10.13140/RG.2.2.16867.99361>
- 647 Peng, Z., Jimenez, J.L., 2021. Exhaled CO<sub>2</sub> as a COVID-19 infection risk proxy for different  
648 indoor environments and activities. *Environ Sci Technol Lett* 8, 392–397.  
649 <https://doi.org/10.1021/acs.estlett.1c00183>
- 650 Peng, Z., Rojas, A. L. P., Kropff, E., Bahnfleth, W., Buonanno, G., Dancer, S. J., Kurnitski, J.,  
651 Li, Y., Loomans, M. G. L. C., Marr, L. C., Morawska, L., Nazaroff, W., Noakes, C., Querol,  
652 X., Sekhar, C., Tellier, R., Greenhalgh, T., Bourouiba, L., Boerstra, A., Tang, J. W., Miller,  
653 S. L., and Jimenez, J. L.: Practical Indicators for Risk of Airborne Transmission in Shared  
654 Indoor Environments and Their Application to COVID-19 Outbreaks, *Environ. Sci.*  
655 *Technol.*, 56, 1125-1137, 2022.
- 656 Persily, A., de Jonge, L., 2017. Carbon dioxide generation rates for building occupants. *Indoor*  
657 *Air* 27, 868–879. <https://doi.org/10.1111/ina.12383>
- 658 Persily, A., Bahnfleth, W., Kipen, H., Lau, J., Mandin, C., Sekhar, C., Wagoocki, P. and Nguyen  
659 Weekes, L., 2022, ASHRAE's New Position Document on Indoor Carbon  
660 Dioxide, *ASHRAE Journal*,  
661 [https://tsapps.nist.gov/publication/get\\_pdf.cfm?pub\\_id=934476](https://tsapps.nist.gov/publication/get_pdf.cfm?pub_id=934476)
- 662 Riley, E. C., Murphy, G., Riley, R. L., 1978. Airborne spread of measles in a suburban  
663 elementary school. *American journal of epidemiology*, 107(5), 421–432.  
664 <https://doi.org/10.1093/oxfordjournals.aje.a112560>
- 665 Pollock, A.M., Lancaster, J., 2020. Asymptomatic transmission of covid-19. *The BMJ*.  
666 <https://doi.org/10.1136/bmj.m4851>
- 667 Pouwels, K.B., et al., 2021. Community prevalence of SARS-CoV-2 in England from April to  
668 November, 2020: results from the ONS Coronavirus Infection Survey. *The Lancet Public*  
669 *Health* 6, e30–e38. [https://doi.org/10.1016/S2468-2667\(20\)30282-6](https://doi.org/10.1016/S2468-2667(20)30282-6)
- 670 Qian, H., Miao, T., Liu, L., Zheng, X., Luo, D., Li, Y., 2021. Indoor transmission of SARS-  
671 CoV-2. *Indoor Air* 31, 639–645. <https://doi.org/10.1111/ina.12766>
- 672 Rudnick, S.N., Milton, D.K., 2003. Risk of indoor airborne infection transmission estimated  
673 from carbon dioxide concentration. *Indoor Air* 13, 237–245.  
674 <https://doi.org/10.1034/j.1600-0668.2003.00189.x>

- 675 REHVA, 2021. REHVA COVID-19 Guidance, version 4.1. Brussels, Belgium: Federation of  
676 European Heating, Ventilation and Air Conditioning Associations.  
677 [https://www.rehva.eu/fileadmin/user\\_upload/REHVA\\_COVID-](https://www.rehva.eu/fileadmin/user_upload/REHVA_COVID-19_guidance_document_V4.1_15042021.pdf)  
678 [19\\_guidance\\_document\\_V4.1\\_15042021.pdf](https://www.rehva.eu/fileadmin/user_upload/REHVA_COVID-19_guidance_document_V4.1_15042021.pdf)
- 679 Richardson, E.T., Morrow, C.D., Kalil, D.B., Bekker, L.G., Wood, R., 2014. Shared air: A  
680 renewed focus on ventilation for the prevention of tuberculosis transmission. *PLoS One*  
681 *9*, 1–7. <https://doi.org/10.1371/journal.pone.0096334>
- 682 SAGE-EMG, 2020. EMG: Role of ventilation in controlling SARS-CoV-2 transmission.  
683 [https://www.gov.uk/government/publications/emg-role-of-ventilation-in-controllingsars-](https://www.gov.uk/government/publications/emg-role-of-ventilation-in-controllingsars-cov-2-transmission-30-september-2020)  
684 [cov-2-transmission-30-september-2020](https://www.gov.uk/government/publications/emg-role-of-ventilation-in-controllingsars-cov-2-transmission-30-september-2020)
- 685 Shen, J., Kong, M., Dong, B., Birnkrant, M.J., Zhang, J., 2021. A systematic approach to  
686 estimating the effectiveness of multi-scale IAQ strategies for reducing the risk of airborne  
687 infection of SARS-CoV-2. *Build Environ* *200*.  
688 <https://doi.org/10.1016/j.buildenv.2021.107926>
- 689 Sobol', I.M., 1994. *A Primer for the Monte Carlo Method* (1st ed.). CRC Press.  
690 <https://doi.org/10.1201/9781315136448>
- 691 Su, A., Grist, S.M., Geldert, A., Gopal, A., Herr, A.E., 2021. Quantitative UV-C dose validation  
692 with photochromic indicators for informed N95 emergency decontamination. *PLoS ONE*  
693 *16*, 1–24. <https://doi.org/10.1371/journal.pone.0243554>
- 694 van Doremalen, N., Bushmaker, T., Morris, D.H., Holbrook, M.G., Gamble, A., Williamson,  
695 B.N., Tamin, A., Harcourt, J.L., Thornburg, N.J., Gerber, S.I., Lloyd-Smith, J.O., de Wit,  
696 E., Munster, V.J., 2020. Aerosol and Surface Stability of SARS-CoV-2 as Compared with  
697 SARS-CoV-1. *New England Journal of Medicine* *382*, 1564–1567.  
698 <https://doi.org/10.1056/nejmc2004973>
- 699 Vouriot, C.V.M., Burridge, H.C., Noakes, C.J., Linden, P.F., 2021. Seasonal variation in  
700 airborne infection risk in schools due to changes in ventilation inferred from monitored  
701 carbon dioxide. *Indoor Air* *31*, 1154–1163. <https://doi.org/10.1111/ina.12818>
- 702 Wagner, J., Sparks, T.L., Miller, S., Chen, W., Macher, J.M., Waldman, J.M., 2021. Modeling  
703 the impacts of physical distancing and other exposure determinants on aerosol  
704 transmission. *J Occup Environ Hyg* *1–15*.  
705 <https://doi.org/10.1080/15459624.2021.1963445>
- 706 Wei, J., Li, Y., 2016. Airborne spread of infectious agents in the indoor environment. *Am J*  
707 *Infect Control* *44*, S102–S108. <https://doi.org/10.1016/j.ajic.2016.06.003>
- 708 Wood, R., Morrow, C., Ginsberg, S., Piccoli, E., Kalil, D., Sassi, A., Walensky, R.P., Andrews,  
709 J.R., 2014. Quantification of shared air: A Social and environmental determinant of  
710 airborne disease transmission. *PLoS One* *9*, 1–8.  
711 <https://doi.org/10.1371/journal.pone.0106622>
- 712 Zhang, S., Ai, Z., Lin, Z., 2021. Occupancy-aided ventilation for both airborne infection risk  
713 control and work productivity. *Build Environ* *188*.  
714 <https://doi.org/10.1016/j.buildenv.2020.107506>
- 715 Zhang, S., Niu, D., Lin, Z., 2022. Occupancy-aided ventilation for airborne infection risk  
716 control: Continuously or intermittently reduced occupancies? *Build Simul*.  
717 <https://doi.org/10.1007/s12273-022-0951-7>
- 718 Zürcher, K., Morrow, C., Riou, J., Ballif, M., Koch, A.S., Bertschinger, S., Liu, X., Sharma,

719 M., Middelkoop, K., Warner, D., Wood, R., Egger, M., Fenner, L., 2020. Novel approach  
 720 to estimate tuberculosis transmission in primary care clinics in sub-Saharan Africa:  
 721 Protocol of a prospective study. *BMJ Open* 10. [https://doi.org/10.1136/bmjopen-2019-](https://doi.org/10.1136/bmjopen-2019-036214)  
 722 036214  
 723

## 724 Supplementary Information

### 725 Derivation Process for Scenario 1 and Scenario 2

726 Scenario 1 and Scenario 2 have constant infection ratios among different occupancy stages, specifically,  
 727  $I_1/N_1 = I_2/N_2 = \dots = I_i/N_i$ .

728 For  $S_1$  (the start occupancy stage) with no initial quanta and initial excess  $CO_2$ , the solved quanta  
 729 concentration ( $C_{q,1}$ ) and excess  $CO_2$  concentration ( $C_{CO2,1}$ ) over time  $T_1$  through mass balance equations can  
 730 be expressed as:

$$731 \quad C_{q,1}(t) = -\frac{I_1 E_q}{\lambda_1 V} e^{-\lambda_1 t} + \frac{I_1 E_q}{\lambda_1 V} \quad (S1)$$

$$732 \quad C_{CO2,1}(t) = -\frac{N_1 E_{CO2}}{\lambda_1 V} e^{-\lambda_1 t} + \frac{N_1 E_{CO2}}{\lambda_1 V} \quad (S2)$$

733 A fixed proportion between quanta and excess  $CO_2$  during stage  $S_1$  can be derived:

$$734 \quad \frac{C_{q,1}(t)}{C_{CO2,1}(t)} = \frac{I_1 E_q}{N_1 E_{CO2}} \quad (S3)$$

735 Because initial quanta concentration ( $C_{qin,2}$ ) and initial excess  $CO_2$  concentration ( $C_{cin,2}$ ) for next  
 736 occupancy stage  $S_2$  are exactly the concentrations at the end of  $S_1$ , thus, they also have the fixed proportion  
 737 relationship as:

$$738 \quad \frac{C_{qin,2}(t)}{C_{cin,2}(t)} = \frac{I_1 E_q}{N_1 E_{CO2}} \quad (S4)$$

739 For  $S_2$  (second occupancy stage), replacing initial quanta concentration ( $C_{qin,2}$ ) by initial excess  $CO_2$   
 740 concentration ( $C_{cin,2}$ ) on basis of the fixed proportion above and a constant infection ratio of  $I_1/N_1 = I_2/N_2$ ,  
 741 quanta concentration and excess  $CO_2$  concentration over time ( $T_2$ ) can be expressed as:

$$742 \quad C_{q,2}(t) = \frac{I_2 E_q}{N_2 E_{CO2}} \left( (C_{cin,2} - \frac{N_2 E_{CO2}}{\lambda_2 V}) e^{-\lambda_2 t} + \frac{N_2 E_{CO2}}{\lambda_2 V} \right) \quad (S5)$$

$$743 \quad C_{CO2,2}(t) = \left( (C_{cin,2} - \frac{N_2 E_{CO2}}{\lambda_2 V}) e^{-\lambda_2 t} + \frac{N_2 E_{CO2}}{\lambda_2 V} \right) \quad (S6)$$

744 A same proportion between quanta and excess  $CO_2$  concentration can be found during occupancy stage  
 745  $S_2$ :

$$746 \quad \frac{C_{q,2}(t)}{C_{CO2,2}(t)} = \frac{I_2 E_q}{N_2 E_{CO2}} \quad (S7)$$

747 If there exists a stage  $S_0$  following stage  $S_2$  that without occupancy (no occupants indoor during period  
 748  $T_0$ ), quanta and excess  $CO_2$  remained by stage  $S_2$  also experience a synchronously damping in fixed  
 749 proportion as  $S_2$ :

$$750 \quad C_{q,0}(t) = \frac{I_2 E_q}{N_2 E_{CO2}} (C_{cin,0} e^{-\lambda_0 t}) \quad (S8)$$

$$751 \quad C_{CO2,0}(t) = C_{cin,0} e^{-\lambda_0 t} \quad (S9)$$

$$752 \quad \frac{C_{q,0}(t)}{C_{CO2,0}(t)} = \frac{I_2 E_q}{N_2 E_{CO2}} \quad (S10)$$

753 Based on constant infection ratios ( $I_1/N_1 = I_2/N_2 = \dots = I_i/N_i$ ), a general analytical expression for quanta

754 concentration and excess  $CO_2$  concentration for stage  $S_i$  can be concluded from the derivation process above:

$$755 \quad C_{q,i}(t) = \frac{I_i}{N_i} \frac{E_q}{E_{CO_2}} \left( (C_{cin,i} - \frac{N_i E_{CO_2}}{\lambda_i V}) e^{-\lambda_i t} + \frac{N_i E_{CO_2}}{\lambda_i V} \right) \quad (S11)$$

$$756 \quad C_{CO_2,i}(t) = (C_{cin,i} - \frac{N_i E_{CO_2}}{\lambda_i V}) e^{-\lambda_i t} + \frac{N_i E_{CO_2}}{\lambda_i V} \quad (S12)$$

757 For all occupancy stages in Scenario 1 and Scenario 2, quanta concentration and excess  $CO_2$  concentration  
758 possess a fixed proportion dominated by three parameters: (1) constant infection ratio; (2) constant quanta  
759 emission rate; (2) constant  $CO_2$  emission rate.

$$760 \quad \frac{C_{q,i}(t)}{C_{CO_2,i}(t)} = \frac{I_i}{N_i} \frac{E_q}{E_{CO_2}} \quad (S13)$$

761 Replacing quanta concentration by excess  $CO_2$  concentration, airborne infection risk for stage  $i$  can be  
762 quantified through Wells-Riley equation based on the excess  $CO_2$  concentration:

$$763 \quad P = 1 - e^{-B \frac{I_i E_q}{N_i E_{CO_2}} \int_0^{T_i} C_{CO_2,i}(t) dt} \quad (S14)$$

764 Equation (S14) can be converted directly into the classical rebreathed fraction-based infection risk model  
765 (Rudnick and Milton, 2003) with  $BC_{CO_2}(t)/E_{CO_2}$  representing the rebreathed fraction. Safe excess  $CO_2$   
766 threshold for occupancy stage  $S_i$  for Scenario 1 and Scenario 2 ( $I_i/N_i = P_i$ ) can then be derived on basis of  
767 Equation (S14) with a predefined risk threshold  $P_i$ :

$$768 \quad C_t = \frac{E_{CO_2} N_i}{E_q T_i B I_i} \ln \left( \frac{1}{1 - P_t} \right) \quad (S15)$$

769 For each occupancy stage, the initial quanta released by previous stages has been considered in the  
770 derivation of safe excess  $CO_2$  threshold in Equation (S15). The application of the derived  $CO_2$  threshold can  
771 be extended to more general occupancy stages without limitation of no initial quanta in space.

772

## 773 Reference

774 Rudnick, S.N., Milton, D.K., 2003. Risk of indoor airborne infection transmission estimated from carbon  
775 dioxide concentration. *Indoor Air* 13, 237–245. <https://doi.org/10.1034/j.1600-0668.2003.00189.x>

776

777

778

779

780

781

782

783

## Highlights

- Rebreathed fraction-based model can be applied for spaces with changing occupants but constant infection ratios.
- Initial quanta and excess  $CO_2$  lead to bias of determining excess  $CO_2$  threshold when infection ratio changes.
- Excess  $CO_2$  threshold contains large uncertainty and should be determined on a case-by-case basis.

Journal Pre-proof

**Declaration of interests**

The authors declare that they have no known competing financial interests or personal relationships that could have appeared to influence the work reported in this paper.

The authors declare the following financial interests/personal relationships which may be considered as potential competing interests:

Xiaowei Lyu reports financial support was provided by China Scholarship Council.

Journal Pre-proof